Mechanical Enhancement of Cellulose Nanofibril (CNF) Films Through the Addition of Water-soluble Polymers

Endrina Stefani Forti
Purdue University
Sami M El Awad
Purdue University
Xin Y Ng
Purdue University
Whirang Cho
American University
Gregory T Schueneman
USDA Forest Products Laboratory
Robert J Moon
USDA Forest Products Laboratory
Douglas M Fox
American University
Jeffrey Youngblood (jpyoungb@purdue.edu)
Purdue University https://orcid.org/0000-0002-8720-8642

Research Article

Keywords: Cellulose Nanofibers, Polyvinyl alcohol, Poly(2-ethyl-2-oxazoline), Tensile properties, Composite film

Posted Date: March 8th, 2021

DOI: https://doi.org/10.21203/rs.3.rs-162652/v1

Abstract

In this work, water-soluble polymers were screened through solution casting and polyvinyl alcohol (PVA) and *poly(2-ethyl-2-oxazoline)* (PEOX) were found as reinforcement agents for cellulose nanofibrils (CNFs) films. Mechanical property increases of 99% in elastic modulus, 93% in the ultimate tensile strength (UTS) and 134% in the work of failure (WOF) were reported for TEMPO-oxidized cellulose nanofibrils (TOCNF) with 0.44 mmol/g carboxylate groups and 15 wt.% PVA. PEOX had a higher elastic modulus increase of 113%, yet lower UTS and WOF increases were found at 63% and 28%, respectively. Additionally, increases in UTS and elastic modulus were also seen in mechanically fibrillated CNF and TOCNFs with higher carboxylate contents (1.5 mmol/g). The toughening mechanism was attributed to the formation of strong hydrogen bonding between the CNFs and the hydrophilic polymers added. The presence of such mechanisms was indirectly confirmed by tensile testing, zeta potential and rheology.

Introduction

Cellulose nanofibers (CNF) are polysaccharide nanomaterials that can be harvested from numerous sources including wood, plants, and other biomass (Isogai et al. 2011; Moon et al. 2011; Clarkson et al. 2020). These materials are inherently sustainable, bio-renewable and non-toxic. Additionally, their uniform widths, high crystallinity, and large aspect ratios make them attractive reinforcing materials. Two approaches are generally used to isolate CNFs. The first one requires fibrillation of cellulosic slurries in a disc refiner or high-pressure homogenizer. The extracted CNF, sometimes called cellulose microfibrils (CMF), has a white appearance and is constituted by larger and more aggregated fibrils. Here we will refer to this as mCNF for mechanical CNF to distinguish this from the broader classification of CNF. Generally, mCNF films exhibit a semi-ductile behavior with strain ratios that can reach the 10% mark and UTS values around 200 MPa (Moon et al. 2011; Benítez and Walther 2017; El Awad Azrak et al. 2019). A chemically oxidative process can also be employed to isolate CNFs products which involve the use of oxidants such as 2,2,6,6 tetramethylpiperidine-1-oxyl radical (TEMPO) to produce a more stable suspension of fibrils (i.e., increased dispersion) and facilitate fibrillation. TEMPO-oxidized cellulose nanofibrils or TOCNFs are constituted by 2–3 nm wide fibrils with reduced adhesion between them, generating a transparent suspension with outstanding mechanical properties. TOCNF films have been reported with an elastic modulus of up to 20GPa and UTS of up to 300 MPa while sustaining a more brittle behavior than mCNF (Saito et al. 2007, 2009; Fukuzumi et al. 2009; Isogai et al. 2011; Moon et al. 2011; Fujisawa et al. 2011; Benítez and Walther 2017; Forti et al. 2020).

An important application of both types of CNFs has been found in their use as reinforcing agents in biodegradable polymers. The strategy often generates films or fibers with improved mechanical performance (> 30%) and environmentally friendliness (Iwatake et al. 2008; Jonoobi et al. 2010; Liu et al. 2013; Rowe et al. 2016; Nair et al. 2017; Meng et al. 2018; Li et al. 2018; Clarkson et al. 2019). Although the reported literature has been successful at processing more biofriendly nanocomposites, there is a lack of literature concerning the development of nanocomposites with higher CNF content (> 20 wt.%). For instance, Kurihara et al. (2015) used poly(acrylamide) (PAM) to produce transparent films with higher

mechanical properties when the polymer was added in the 10–25 wt% range into TOCNF. Another example can be found in the work performed by Hakalahti et al. (2015) whereby adding polyvinyl alcohol (PVA) to TOCNF solutions, they produced films that were stable in wet conditions. However, a robust study of other polymers has yet to be investigated for reinforcement in high CNF content nanocomposites (Kurihara and Isogai 2015; Hakalahti et al. 2017).

To address this knowledge gap, we utilized solution casting as a simple yet reliable method to process nanocomposite films of CNF containing small concentrations (5 to 20 wt.%) of a variety of water-soluble polymers to investigate whether they can act as mechanical property enhancing additives. The addition of PVA and poly(2-ethyl-2-oxazoline) (PEOX) generated remarkable improvements in the UTS and Young's modulus of TOCNF films while maintaining their transparency. Therefore, special attention was dedicated to assessing the effects of varying the molecular weight, hydrolysis degree and concentration of these polymers in the TOCNF mechanical properties. To elucidate the nature of the polymer interactions, zeta potential, and capillary rheology analysis were performed. Finally, to prove the efficacy of the method with different CNF types, the same concentrations of PVA and PEOX were added to mCNF solutions, where a significant increase in the mechanical properties and similar trends were observed. The outstanding mechanical increases achieved open a wide window for potential application of these films in future light-weighted and high-performance renewable materials.

Materials And Methods

Materials

Two different TOCNF suspensions produced by USDA Forest-Service-Forest Products Laboratory (FPL), Madison, WI, USA and purchased from the University of Maine were used. TOCNF (lot #2019-FPL-CNF-139) was prepared using sodium chlorite at pH 7 with a carboxylic content of 0.44 mmol/g (Saito et al. 2007). TOCNF (lot #2018-FPL-CNF-129) was prepared using the sodium hypochlorite method at pH 10 and had a carboxylic content of 1.5 mmol/g (Saito et al. 2009). Both materials will be denominated c-TOCNF and h-TOCNF respectively to avoid confusion during the discussion. Additionally, a mCNF slurry with a solid concentration of 3 wt.% was also purchased from the same vendor (lot CNF, Batch #103). Additionally, several water-soluble polymers were obtained from different vendors and can be seen in Table 1.

Table 1
Water-soluble polymers purchased from different suppliers along with molecular weight and hydrolyzation (%)

Polymer	Abbreviation	Manufacturer	Lot number (#)	Molecular weight (g/mol)	Hydrolyzation (%)
Poly(vinyl alcohol)	PVA 85–124 99%H	Sigma-Aldrich	MKBS2768V	85,000-124,000	99
Poly(vinyl alcohol)	PVA 146–186 99%H	Sigma-Aldrich	MKCC7856	146,000-186,000	99
Poly(vinyl alcohol)	PVA 146–186 87–89%H	Sigma-Aldrich	MKBX9187V	146,000-186,000	87–89
Poly(2-ethyl-2-oxazoline)	PEOX 50	Sigma-Aldrich	04629JJ	50,000	-
Poly(2-ethyl-2-oxazoline)	PEOX 200	Sigma-Aldrich	MKCC1604	200,000	-
Poly(2-ethyl-2-oxazoline)	PEOX 500	Sigma-Aldrich	MKBX0709V	500,000	-
Poly(acrylamide-co-acrylic acid)	PAMA	Sigma-Aldrich	02312LE	5,000,000	-
Poly(2-hydroxymethyl methacrylate)	PHEMA	Sigma-Aldrich	12801TC	300,000	-
Methyl 2-hydroxyethyl cellulose	MHEC	Sigma-Aldrich	MKBX7592V	130	-
Poly(ethylene oxide)	PEO	Sigma-Aldrich	05010KH	1,000,000	-
Polyvinylpyrrolidone	PVP	Fluka Analytical	BCBF3274V	360,000	-

Fabrication of nanocomposite films

TOCNF suspensions in water were diluted with deionized water to 0.53 wt%. Water-soluble polymers were added in concentrations ranging from 5–20 wt.% (dry weight relative to TOCNF). The mix was stirred at different temperatures to promote the dissolution of the polymers in water. The solutions were later cast into 90 mm polystyrene Petri dishes as reported in previous studies (Moon et al. 2011). To obtain films with approximately the same thicknesses, 50 ml of the solution was cast. The cast solutions were placed in a humidity chamber with a fixed relative humidity of 50% at room temperature (~ 21 °C). Films were

completely dry after 7 days with an average thickness of 30 μm ± 2. After drying, the films were removed from the Petri dish by cutting the edges of the film with a razor blade and slowly detaching them with the help of tape.

In the case of mCNF films, water-soluble polymers were first diluted in deionized water with mild heating (90 °C) mechanical stirring. Once dissolved, the polymeric solutions were added to a 3 wt.% mCNF suspension in water and mixed using a planetary centrifugal mixer (DAC 400.1 FVZ, FlackTek Inc., Landrum, SC, USA) at 2500 rpm for a total time of 2 minutes. The mixture was then cast into 90 mm Petri dishes and dried in a fixed relative humidity of 50% at room temperature (~ 21 °C). The films were completely dry after 7 days and were detached with the help of tape and scissors. Table 2 shows a detailed composition of the samples prepared for mCNF, c-TOCNF, and h-TOCNF.

Table 2
Composition of films produced

Polymer		**Weight percentage (%)**			
Matrix	**Water-soluble polymer**	**5**	**10**	**15**	**20**
c-TOCNF	PVA 85–124 99%H	□	□	□	□
	PVA 146–186 99%H	□	□	□	□
	PVA 146–186 87–89%H	□	□	□	□
	PEOX 50	□	□	□	-
	PEOX 200	□	□	□	-
	PEOX 500	□	□	□	-
	PAMA	-	□	-	-
	PHEMA	-	□	-	-
	MHEC	-	□	-	-
	PEO	-	□	-	-
	PVP	-	□	-	-
h-TOCNF	PVA 146–186 99%H	□	□	□	-
	PEOX 200	□	□	□	-
mCNF	PVA 146–186 99%H	-	□	□	-
	PEOX 200	-	□	□	-

Tensile testing

A laser cutter (Muse Hobby Laser Cutter, Full Spectrum Laser, Las Vegas, NV, USA) was used to obtain 1:5 scale dogbone-shaped specimens of ~ 0.8 mm width and ~ 6.5 mm of gauge length according to the ASTM D638 Standard Test Method for Tensile Properties of Plastics. Samples were tested in a dynamic mechanical analyzer (DMA) (Q850 TA instruments New Castle, DE, USA), using the rate-controlled stress ramp mode fixed at a 1 N/min displacement rate. TOCNF specimens had an average thickness of 40 ± 3 μm while mCNF specimens had an average thickness of 74 ± 5 μm. Samples were conditioned in a low humidity chamber (25% RH) for three days at room temperature before testing. A minimum of 5 specimens were tested at room temperature (24 °C) and 35% RH. Young's modulus was determined from the maximum slope of the stress-strain curve, ultimate tensile strength (UTS) was taken as the highest tensile stress on the stress-strain curve, while the work-of-failure (WOF) was calculated by integrating the area under the stress-strain curve. Analyses of variance (ANOVA) were conducted to compare results, at a threshold level of 0.05.

Transmission Electron Microscopy (TEM)

A 0.1 wt% TOCNF solution was dropped onto a 200 mesh Formvar/Carbon coated Cu grid. After 20 s, the excess liquid was wicked using an ashless Whatman filter paper. The grids were then stained with 0.5 % gadolinium(III) acetate for 2 min and dried before imaging. Transmission electron microscopy (TEM) images were taken using a JEOL JEM-2100 Plus with an accelerating voltage at 200 kV. Images were taken at 50,000x magnification with a resolution of 0.255 nm/pixel. The image size was calibrated using a 500 nm gold grid diffraction grating. Fiber widths were measured using a custom ImageJ macro (Meija et al. 2020).

Zeta potential

Solutions (Table 2) were diluted to 0.1 wt% solids using deionized water. At least 5 measurements of each sample were obtained using a Zetasizer Nano Series (Malvern Instruments, MA, USA) in z-potential mode at room temperature (24 °C). Analyses of variance (ANOVA) were conducted to compare results, at a threshold level of 0.05.

UV-Vis Spectroscopy

Optical absorbance was measured by UV-Vis spectroscopy (UV–Vis spectrophotometer Spectramax Plus 384, Molecular devices Corp., Sunnyvale, CA) in the wavelength range from 400 to 750 nm with air as the background. Transmission data was normalized by the sample thickness for comparison purposes.

Rheometry

The shear rheological behavior of solutions was analyzed using a Bohlin Gemini HR nano Rheometer (Malvern Instruments, MA, USA) with a 40 mm serrated parallel plate configuration with a 1 mm gap to avoid wall depletion effects. An ABS vapor-trap device with a wet sponge was used to minimize moisture loss of the samples during testing (Montes et al. 2020). A pre shear of 1000 s^{-1} was applied to all the samples for 30 seconds. The experiment was set to run a shear stress ramp of 40 logarithmic increment steps from a min shear rate of 0.1 s^{-1} to 500 s^{-1}. All tests were run at room temperature (25 °C).

Fourier Transform Infrared Spectroscopy (FTIR)

Films were subjected to FT-IR analysis using a (Spectrum 100, PerkinElmer, MA, USA). All spectra were collected with 10 scans of 4000 to 600 cm^{-1} with a resolution of 4 cm^{-1}. All samples were subjected to dry condition environments for a minimum of 3 days at 15% RH.

Results And Discussion

Processing

Water-soluble polymers were chosen due to their ease of dispersion in water CNF solutions, leading to maximized interactions between fibrils and polymeric chains. Solution casting was chosen as it is a simple and reliable method to process CNF films with high dispersion. In the case of TOCNFs, the solutions were diluted and easily mixed using a stirrer plate and low temperatures. In all cases, the temperature was kept below 90 °C for less than two hours to achieve the total dissolution of the polymers in the TOCNF solution. All films were left to dry inside a humidity chamber with a controlled relative humidity of 50% and detached after 7 days for further inspection. Self-standing composite films produced were flat, highly transparent with no appreciated haziness and smooth surfaces (Fig. 1). Furthermore, films were glossy and flexible as can be seen in Fig SI1 of supplemental information. Characteristic plots of transmittance obtained by UV-Vis is shown in Fig. 2. Overall, both the TOCNF and composite films showed a small decrease in transparency when compared with silica glass. The normalized transmittance shows a 10% lower transmittance of neat TOCNF films in the blue range when compared with silica glass. The difference is reduced at long (red) wavelengths reaching a difference of less than 2% at the 700 nm wavelength. TOCNF + PVA composites' behavior showed a similar trend to neat TOCNF, with a slight decrease in transparency through all the regions. In contrast, PEOX composites showed a better transmittance than neat TOCNF in the blue regions, maintaining transparency throughout the spectrum. While TOCNF has been known to have a slight yellow/brown color explaining the small loss in transparency that is magnified in the blue region, it is not clear why composites differ as both PVA and PEOX have extremely high transparency in this region. However, differences may be related to small variations in dispersion of the TOCNF upon adding the polymers. Regardless, the loss of transparency is not noticeable to the naked eye.

Mechanical Properties

Water-soluble polymers

A wide range of polymers were added to c-TOCNF at an initial concentration of 10 wt%. Films produced were tested in tension until failure in a DMA. The mechanical response can be observed in Table 3.

Table 3
Tensile response of TOCNF films with 10 wt% addition of water-soluble polymers

Samples	UTS (MPa)	Young's Modulus (GPa)	WOF (MJ/m^3)
Neat c-TOCNF	163 ± 16	13 ± 2	1.6 ± 0.3
c-TOCNF + 10 wt% PAMA	184 ± 25	16 ± 1	2.6 ± 0.6
c-TOCNF + 10 wt% PHEMA	183 ± 19	16 ± 1	2.3 ± 0.5
c-TOCNF + 10 wt% PVP	189 ± 12	15 ± 1	2.6 ± 0.5
c-TOCNF + 10 wt% MHEC	191 ± 15	11 ± 1	3.4 ± 0.5
c-TOCNF + 10 wt% PEO	189 ± 17	11 ± 2	2.4 ± 0.6
c-TOCNF + 10 wt% PVA 85–124 99% RH	302 ± 10	25 ± 1	3.8 ± 0.7
c-TOCNF + 10 wt% PEOX 500	267 ± 18	28 ± 1	2.1 ± 0.4

Most of the water-soluble composite films achieved increased mechanical properties when compared with neat c-TOCNF films. The increment in some of the properties constitutes in itself an indirect indication of the binding capabilities of water-soluble polymers with TOCNF fibrils. In fact, such an increase has previously been reported in literature. In the work performed by Kurihara et al. (2015) poly(acrylamide) (PAM) was mixed into TOCNF solutions, achieving a mechanical increase in the films when added in the compositions ranging from 10 to 25 wt%. The effect was attributed to the filling or covering of the boundary of the TOCNF domains by PAM (Kurihara and Isogai 2015). An explanation for this reinforcement was schematized by Kurihara et al (2015) based in previous findings reported by Saito et al. (2011). According to the authors, TOCNF in solution forms randomly distributed elements with self-aligned and nematic-ordered structures inside small domains or clusters. Once dry, TOCNF films exhibit an oriented strand board (OSB) structure as can be seen in Fig SI2 (a). When polymers such as PAM are added in small concentrations, they aggregate in the boundary regions of the domains (Fig SI2 (b)). This aggregation serves as a bridge between domains, increasing the mechanical properties of the material. If the concentration of polymer keeps increasing and surpasses a critical value, TOCNF fibrils do not form self-aligned elements, and instead, get distributed in a polymeric matrix, decreasing the mechanical properties of the films (Saito et al. 2011; Kurihara and Isogai 2015).

In this study, PAMA, a polymer with a similar structure was studied. Nevertheless, the mechanical increases achieved by the inclusion of the polymer were not substantial when compared with values reported by Kurihara et al (2015). Similarly, other polymers exhibited similar mechanical increases, such is the case of PHEMA and PVP, two water-soluble polymers that are usually used in the biomedical industry. Other water-soluble polymers tested, and highlighted in blue in Table 3, showed an increased UTS and WOF while the elastic modulus remained within the range of neat c-TOCNF. Such was the case of PEO and MHEC. The hydrogen bonding formation of both polymers is well described in the literature

(Rondo et al. 1994; Khutoryanskaya et al. 2005). Nevertheless, the small increases in UTS and WOF seem to indicate that those interactions may not be responsible for the increased toughness of the films.

Out of all water-soluble polymers tested, PVA 85–124 99%H and PEOX 500 presented exceptional mechanical increases in the films. Tensile testing results indicated an increase of 85% and 63% respectively for UTS. Young's modulus was enhanced by 92% in the case of PVA and 115% with the addition of PEOX. Finally, the WOF of the films showed more than 100% increase. Therefore, special attention was given to the interaction between CNF and these polymers.

c-TOCNF + PVA and PEOX

PVA is one of the highest volume semicrystalline, nontoxic, water-soluble polymers produced in the world (Liu et al. 2013). PVA is used in a wide range of applications like adhesives, packaging materials, films and medical products (Rowe et al. 2016). Many applications of PVA takes advantage of the hydroxyl groups in its chemical structure (Fig SI3 (a)), that are responsible for the binding interactions of PVA with a high number of polymers. Usually, the degree of solubility and some physical properties of PVA can be controlled by varying the molecular weight and degree of hydrolysis of the PVA (Roohani et al. 2008). Likewise, PEOX is a low cytotoxicity polymer with good light stability and re-solubility. The PEOX structure contains a substituted amide group (Fig SI3 (b), that polymerizes by cationic ring-opening polymerization (Zhang et al. 2018). PEOX is suspected to form hydrogen-bonded complexes with polymers containing proton donating groups (Lin et al. 1988).

To further understand the mechanical increase achieved by the addition of PVA and PEOX to the c-TOCNF matrix, two different PVAs were selected with different molecular weights and hydrolysis degrees. In like manner, two molecular weighs for PEOX were selected. Further information about the specific molecular weight and hydrolysis of the PVAs and PEOX can be found in Table 1 on the materials and methods section. Overall, the tensile stress-strain behavior of these six different polymers were studied in a wide range of compositions ranging from 0 to 20 wt% in TOCNF. Fig SI4 on the supplemental information of this paper shows characteristic curves for the neat c-TOCNF, PVA and PEOX. Overall, PVA showed a higher elongation (> 50%), in which case the polymer can yield and plastically deform until failure. Contrarily, PEOX behaved in a brittle manner, failing before reaching the yield point. To simplify this discussion, and due to the different mechanical behavior of both polymers, TOCNF – PVA and TOCNF - PEOX nanocomposites response will be discussed separately in the following sections.

c-TOCNFs + PVA nanocomposites

The response of the nanocomposite films containing PVA at different concentrations can be seen in Fig. 5. All trends showed a significant statistical difference according to the variance analysis performed. All the properties measured showed a marked plateau at 15 wt% that continue through 20 wt% with a slight decrease in the mechanical properties. At concentrations higher than 20 wt%, a further decrease of the mechanical properties of the films can be expected, and therefore, higher concentrations of polymer were not considered in this study.

Young's modulus response can be seen in Fig. 5 (a). The hydrolysis degree of PVA has a marked effect on the mechanical properties reported. For instance, nanocomposite films with higher molecular weight (M_w): 146,000–186,000 but lower hydrolysis 87–88 %H, had lower elastic modulus in comparison with the same M_w, but higher hydrolysis 99%H, specially at higher fractions of PVA. This is expected since the tensile modulus of PVA tends to increase as the degree of hydrolysis increases. A good explanation for this behavior derives from the higher number of hydroxyl groups present in the chain, creating a higher amount of strong hydrogen bonds (Roohani et al. 2008). It can be assumed then, that increasing the number of hydroxyl groups in the molecule could translate into a higher number of interactions between c-TOCNFs and PVA, leading to a stiffer material. In the case of the elastic modulus, a higher molecular weight did not make a substantial difference.

Figure 5 (b) shows results of UTS, where some variability on the results can be seen and it is attributed to the brittle behavior of TOCNF films, where defects are randomly sized and distributed in the matrix. The presence of defects in the films produces an amplification of the stress, leading to failure (Forti et al. 2020). In the same manner discussed before, there is a marked increase in the mechanical properties related to the hydrolysis of the polymers, which could relate to the presence of a higher number of hydrogen bonds. An interesting behavior can be observed where a higher molecular weight gives a higher UTS. It can be assumed then that the larger number H-bonding groups found in a longer chain could increase the total interaction between polymer and fibrils, reinforcing the material (Liu et al. 2012).

There is also an apparent increase in the WOF (toughness) of nanocomposite films by the addition of PVA (Fig. 5 (c)). This is expected behavior due to the UTS increase in the films. For materials that fail in a brittle fashion, strength and toughness tend to correlate as a higher peak stress simply increases area under the curve at a constant SOF. The toughness increase was indistinguishable between the different PVA contents. Overall, the addition of pseudoplastic polymers increased the ability of the films to stretch without failing prematurely, reinforcing the films and increasing their stiffness in the elastic region. Increases achieved at 15 wt% loading were higher for the PVA 146–186 99% H with increments of 93% of the UTS, 99% of Young's modulus, and 137% of the WOF. Strong hydrogen bond formation in the nanocomposite films is suspected to have a large influence on the mechanical increase obtained and will be discussed in further sections of this paper.

c-TOCNFs + PEOX nanocomposites

In the same fashion, the tensile response of nanocomposite films with PEOX is shown in Fig. 6. In contrast with PVA nanocomposites, the mechanical response seems to start a plateau after the addition of 5 wt%. After the plateau region, the mechanical response could be expected to decrease. Therefore, compositions higher than 15 wt% were not tested.

Similar to the addition of the PVA, the addition of PEOX generated a notable increase in the mechanical properties of c-TOCNF. Interestingly, while the brittle response of PEOX is drastically different from the ductile response of PVA (Fig SI4), both polymers seem to reinforce c-TOCNF nanocomposites in a similar

manner. As shown in Fig. 6 (a) the elastic response of nanocomposites increased rapidly after 5 wt% loading, reaching a peak at 5 wt% and surpassing the values obtained by the addition of PVA (30GPa in comparison to 26GPa). Addition of PEOX 200 delivered higher modulus than the PEOX 500 and PEOX 50, while the last two showed a no significant difference as dictated by the ANOVA test performed. The reason for this behavior is currently unknown.

In comparison with the UTS response obtained by the addition of 15 wt% PVA 146–186 99%H (314 ± 13 MPa), the addition of PEOXs generated a slightly lower strength as shown in Fig. 6 (b). In this case, the differences in strength of PEOX 500 and PEOX 200 were not significantly different from each other, while the addition of PEOX 50 generated at much smaller UTS for all weight percentages tested. While there are many possible reasons for the underperformance of PEOX 50, it is important to note that tensile properties of neat PEOX 50 could not be performed due to the brittle behavior of the samples as they failed prematurely before testing. Hence a simple rule-of-mixtures approach would indicate that PEOX 50 would have a lower strength.

Finally, WOF results can be observed in Fig. 6(c). While no statistical difference could be observed between points of the same PEOX, there were differences between the different PEOX molecular weights. It seems that even when the mechanical response of neat PEOX is brittle, the addition of the polymer generates a small increase in the WOF response as expected from the increased UTS.

CNFs response to the addition of PVA and PEOX

To determine if the large mechanical property enhancement was conserved across CNF type, PVA 146–186 99%H and PEOX 200 was studied with different types of CNF. Two different TOCNF (h-TOCNF and c-TOCNF) and a purely mechanical CNF (mCNF) were used and nanocomposite films with different concentrations of the polymers were fabricated and tested in a DMA under tension.

The c-TOCNF, which was utilized previously in this work until now, was first developed by Saito et al. (2007). In their studies, they introduced catalytic oxidation of CNF with TEMPO and sodium chlorite at neutral conditions (pH 7) with the resulting fibrils having an average width of 5 nm and at least 2 μm in length. Overall, an oxidation of 1.5 mmol/g was achieved, which correlates to the oxidation of 15% of the primary hydroxyl group in the cellulose and with no aldehyde groups present (Saito et al. 2007). Different from c-TOCNF, h-TOCNF was developed and the first study in a work done by Saito et al. (2009), where instead of using sodium chlorite, the method involved the usage of sodium hypochlorite under basic conditions (pH 10), which usually generates a higher amount of carboxylate groups in the TOCNF, achieving values of 0.78 mmol/g (Saito et al. 2009). In this study, morphological information of the TOCNF fibrils was obtained via TEM (SI5 of the supplemental information). No statistical difference was found between the widths of the different fibrils. Hence, the main difference between the TOCNFs studied here relies in the number of carboxylate groups present in the cellulose structure with h-TOCNF having a high value (1.5 mmol/g) and c-TOCNF having a lower value (0.44 mmol/g). A third CNF that was purely mechanically derived, containing little to no carboxylate was also included in the study. mCNF is directly derived from the high-speed fibrillation of cellulosic slurries. It is composed of larger and more

aggregated fibrils, as a consequence of strong hydrogen bonds between fibrils (SI6 supplemental information).

For each type of CNF, different weigh percentages ranging from 0 to 15 wt% of polymer were added to determine the optimal concentration needed to maximize mechanical properties. In the case of c-TOCNF, the optimal concentration was found approximately 15 wt%, while for -TOCNF was 10 wt%. Plots of tensile properties for h-TOCNF can be found in Fig SI7 in the supplemental information of this paper. For mCNF, both pictures of the mCNF nanocomposites and their mechanical properties in tension can be found in Fig SI8 and Fig SI9. According to the data gathered, 10 wt% was selected as the optimal concentration at which mechanical properties were higher for the mCNF nanocomposites. Figure 7 shows a comparison between the best-performing films (i.e. optimal concentration for each CNF) along with the percentage increase achieved. Figure 8 shows characteristic plots for the neat polymers along with the increased mechanical properties for the films.

As can be seen in Fig. 7, mechanical reinforcement was achieved for all the CNFs. Although there were some distinctive differences between them. The most significant were that the greatest percentage increase was obtained by the addition of 15 wt% of water-soluble polymers (Either PVA 146–186 99%H or PEOX 200) to c-TOCNF and the mCNF had lowest mechanical properties.

It is important to highlight that the introduction of carboxylate groups in the nanofibrils surface has a big impact on the stability and mechanical properties of the films produced. In the work done by Saito et al. (2009), by decreasing the number of carboxylate groups, a higher UTS was achieved (312 MPa instead of 222 MPa) while maintaining the same Young's modulus (Saito et al. 2009). According to the same author, the presence of carboxylate groups plays a role in the individualization of fibrils while producing stable dispersions (high electrostatic repulsions) (Saito et al. 2007). In this work, the neat mechanical properties of c-TOCNF and h-TOCNF can be found in Table SI1 in the supplemental information. Overall, the mechanical performance of c-TOCNF (carboxylate content 0.44 mmol/g) was higher for UTS but lower for Young's modulus when compared with neat h-TOCNF films (carboxylate content 1.5 mmol/g). When polymer reinforcement was added, a larger mechanical reinforcement was achieved for c-TOCNF composites than for h-TOCNF. While the exact mechanism of reinforcement remains unknown, the authors consider that some interactions can be established between TOCNFs and PVA/ PEOX and that such relationships can be related to the carboxylate content of the TOCNF materials used. In general, by decreasing the number of carboxylate groups on the surface (i.e. c-TOCNF – 0.44 mmol/g) more hydroxyl groups in the fibril are available and ready to interact with molecules in the PVA/ PEOX forming hydrogen bonding interactions that can potentially increase the mechanical response of films. In contrast, a higher carboxylic content (i.e. h-TOCNF 1.5 mmol/g) would reduce the potential binding sites, resulting in a smaller percentual increase in the tensile properties.

Following the same logic, mCNFs that have a more branched and an inherently agglomerated morphology with no carboxylic groups did not see the same level of increase when compared to TOCNFs. The agglomerated and branched networks allow for lower fibril-to-polymer interactions and lower overall

properties as well as the non-transparency of the nanocomposite when compared to TOCNFs. That said, there was still an increase in Young's modulus by 63% and 68% with the addition of PVA 146–186 99%H and PEOX 200 respectively (Fig. 7a) when compared to the neat mCNF. Additionally, the UTS increased by 35% and 22% with the addition of PVA 146–186 99%H and PEOX 200 respectively (Fig. 7b). Due to the large standard deviation seen for neat mCNF films, it seems that there was no change in the WOF when PVA 146–186 99%H was added, yet there appears to be a decrease when PEOX 200 was added. The plausible decrease in WOF could originate from the fact that PEOX made the relatively flexible mCNF structure brittle.

Interestingly, a higher percentage (15 wt%) of the polymer was needed to reach the highest properties for c-TOCNF when compared with other CNFs (10 wt%). Likely, the extra amount of hydroxyl groups on the c-TOCNF surface required an extra amount of polymer to fully bond (i.e. more hydrogen bonds equal better mechanical properties).

Zeta potential

Because direct chemical analysis such as FT-IR proved too difficult due to the overlapping of some of the most important peaks, zeta potential (and rheology measurement) was performed to determine any interactions of PVA and PEOX with the CNFs via colloidal stability. Processes such as adsorption can alter the charge state and stability of nanoparticles in solution, thereby indicating whether polymers are attached (Sjöberg et al. 1999). The zeta potential of neat c-TOCNF and PVA/PEOX nanocomposites can be seen in Fig. 10. All trends showed a statistically different behavior according to the analysis of variance performed. Neat c-TOCNF was chosen as a reference point due to the high mechanical property increase achieved. In the plots, neat c-TOCNF shows a negative value of zeta potential, a clear indicator of the negative electrostatic repulsion achieved by the presence of carboxylic groups on the CNF's surface (Saito et al. 2007, 2009; Liu et al. 2015). The addition of different PVAs at different concentrations generated less negative zeta potential values of the solutions even at low PVA content (5%) and tailing upwards (less negative) at high content. The response obtained for c-TOCNF plus PEOX nanocomposites is also shown in Fig. 8 (right). The trends, although different, likewise show a significantly less negative charge at modest polymer addition (5%). However, at higher concentrations of PEOX, a peak in the trend forms, and the zeta potential becomes more negative with further addition of polymer.

The observed reduction in negative charge correlates with a significant shielding effect of the PVA and PEOX on the electronegative surface of fibrils. It is the assumption of the authors, that this indicates adsorption of polymer onto the CNF, even at low contents (5%), which suggests that this interaction may be important for mechanical reinforcement. While there is a reduction of electrostatic repulsion by the addition of PVA and PEOX that could translate into a higher aggregation of fibrils, the amount is small so is unlikely to be deleterious to mechanical properties. However, adsorption of polymer may allow drying to higher degrees before drying induced aggregation takes place due to steric effects, thus increasing density and/or decreasing defect size. Alternatively, the polymers may be bridging CNF fibrils leading to

reinforcement, or some combination of these factors. Regardless, it is likely that the interaction indicated by zeta potential is in some way leading to the increased mechanical properties.

Rheology

Rheology was also performed to elucidate clues to the fibril-polymer chain interactions. Figure 11 compares TOCNF suspensions held at a constant TOCNF concentration of 0.53 wt% (to match initial concentration of casting solutions) with and without an extra 15 wt% polymer added. c-TOCNF was again chosen due to the higher mechanical increase achieved by the incorporation of water-soluble polymers. Logically, when polymer is added to TOCNF solution, if each material is acting independently, then the composite fluid would have a higher viscosity than pure TOCNF. However, if a strong screening interaction occurs, fibrillar interaction in the fluid decreases, and the viscosity may be lower. Hence this is a method to determine if any interactions between polymer and TOCNF are having an effect on polymer chain motion, as opposed to simply happening. Pure polymer solutions for comparison are given to help identify transitions, although concentrations were 5 wt% and 15 wt% for PVA 146–186 99% H and PEOX 200, respectively to keep the viscosity in scale.

The resultant curve for neat TOCNF (Fig. 11 purple triangles) shows characteristics of shear-thinning behavior, as observed in other TOCNF suspensions (Pääkko et al. 2007; Lasseuguette et al. 2008; Naderi et al. 2014; Aaen et al. 2019). In the work performed by Lundahl et al (2018) polarized imaging confirmed that the shear behavior at rates < 100 s^{-1} are caused by wall depletion, whereas at higher shear rates (i.e. >100 s^{-1}) alignment of the fibrils takes place, lowering the viscosity of the solutions (Lundahl et al. 2018). Figure 11 (blue triangles) depicts the rheological behavior of a neat PVA solution with a 5 wt% solids concentration. As mentioned before, PVA is known to form intra an inter chain hydrogen bonding, an effect that increases with the increment in the degree of hydrolysis. Strong PVA-PVA interactions in water, are a plausible explanation for the high viscosity and shear thinning behavior of the solution as describe elsewhere (Briscoe and Luckham 2000). PEOX characteristic behavior is shown in Fig. 11 (red triangles). While the structure is known to participate in the formation of hydrogen bonds with other polymers (Lin et al. 1988; Zhang et al. 2018), literature concerning rheological properties is scarce. The plot shown highlights a marked decrease in the viscosity of the solution when shear is applied at small rates, potentially related to the destruction of PEOX-water structures. Interestedly, at higher shear rates > 1 s^{-1}, all structures are destroyed, and the solution becomes Newtonian.

In the case of TOCNF where PVA/PEOX was added, the same characteristic shear thinning behavior as neat TOCNF was seen. This behavior is expected since TOCNF fibrils have high surface areas and are present in higher concentrations, which allow for strong fibril interactions (hydrogen bonds, entanglements), governing the rheological properties of the solutions. This is confirmed by the behavior of the neat TOCNF and the composite solutions at high shear rates, where all the curves tended to the same viscosity values, which confirms the governing behavior of TOCNF over the presence of small amounts of water-soluble polymers (Lundahl et al. 2018). Most importantly, the viscosity decreases when

small concentrations of PVA were added to the TOCNF solutions at low shear rates as shown in Fig. 11 (blue dots). This is a clear indication of the TOCNF-PVA interactions in water. It is widely accepted in the literature that the interaction between TOCNF fibrils in suspension facilitates the creation of network structures by the creation of hydrogen bonds between fibrils (Iotti et al. 2011). The decreased viscosity achieved by the introduction of PVA seems to indicate a reduced fibril-fibril interaction, giving an indirect indication of possible hydrogen bonding formation between fibrils and PVA (Velásquez-Cock et al. 2018) (Fig SI10 supplemental information) that translates into a reduced viscosity explained by the reduction of fibril structures, allowing a better flow under shear and a decreased viscosity for shear rates < 100 s^{-1}. Practically, this lowered viscosity would allow a higher concentration before the gel-point during drying and reduced residual stress in the films, along with likely, smaller aggregates upon drying.

The case of TOCNF + PEOX is shown in Fig. 11 (red dots), where there is an increased viscosity measured for all ranges of shear until 100 s^{-1} where all trends unify and show similar values of viscosity. While this may indicate less or no interaction between TOCNF and polymer at this concentration, the likelihood of a higher number of interactions happening at higher concentrations (i.e. when films are drying) is still possible. Regardless, as both PVA and PEOX show uniquely high mechanical property increases and similar zeta potential changes, it is likely that some sort of interaction occurs, even if not rheologically determinable.

Conclusion

A wide range of water-soluble polymers were evaluated to enhance the mechanical properties of CNF. The two best performing candidates, PVA and PEOX, were selected for further testing due to the mechanical property increase achieved by the addition of 10 wt% to a TOCNF matrix. Different concentrations (up to 20 wt%) of such polymers in combination with different molecular weighs and hydrolysis degrees were tested. Higher molecular weight generally led to increased properties, although hydrolysis level was the dominant factor in PVA, with higher hydrolysis leading to increased properties. Due to the observed improvement in the mechanical performance of TOCNFs, other CNFs were tested with the two best performing polymers, PVA 146–186 99% H and PEOX 200. An increase of 113% in the modulus, 93% in the UTS, and 134% in the WOF were achieved by c-TOCNFs; 48% in modulus, 93% in UTS, and 98% in WOF for h-TOCNF; and 68% in modulus, 35% in UTS, and a decrease in WOF due to embrittlement in mCNF were observed. Overall, PVA seemed to perform better than PEOX.

The increased mechanical response was attributed to the creation of hydrogen bonds between the CNF fibrils and the hydrophilic polymers added. Zeta potential and rheometry were used as an indirect verification of the creation of such bonds. Zeta potential showed an increase in charge (less negative) for both PVA and PEOX and rheometry showed a decrease in viscosity of TOCNF solution when a small amount of PVA is added indicating that polymer adsorption and screening is likely happening. Overall, the work showed that adding a small amount of polymer can successfully increase mechanical properties across different types of CNF, thereby providing a method to tune properties of this interesting class of materials.

Declarations

Acknowledgments

The authors would like to acknowledge financial support from the Private–Public Partnership for Nanotechnology in the Forestry Sector (P3Nano) under Grant Number 109217.

Author Contributions

The manuscript was written through the contributions of all authors. All authors have approved the final version of the manuscript.

Notes

The author declares no competing financial interest.

References

Aaen R, Simon S, Wernersson Brodin F, Syverud K (2019) The potential of TEMPO-oxidized cellulose nanofibrils as rheology modifiers in food systems. Cellulose 26:5483–5496. https://doi.org/10.1007/s10570-019-02448-3

Benítez AJ, Walther A (2017) Cellulose nanofibril nanopapers and bioinspired nanocomposites: A review to understand the mechanical property space. J. Mater. Chem. A 5:16003–16024

Briscoe B, Luckham P (2000) The effects of hydrogen bonding upon the viscosity of aqueous poly(vinyl alcohol) solutions. Polymer (Guildf) 41:3851–3860. https://doi.org/10.1016/S0032-3861(99)00550-9

Clarkson CM, El Awad Azrak SM, Chowdhury R, et al (2019) Melt Spinning of Cellulose Nanofibril/Polylactic Acid (CNF/PLA) Composite Fibers For High Stiffness. ACS Appl Polym Mater acsapm.8b00030. https://doi.org/10.1021/acsapm.8b00030

Clarkson CM, El Awad Azrak SM, Forti ES, et al (2020) Recent Developments in Cellulose Nanomaterial Composites. Adv Mater 2000718. https://doi.org/10.1002/adma.202000718

El Awad Azrak SM, Clarkson CM, Moon RJ, et al (2019) Wet-Stacking Lamination of Multilayer Mechanically Fibrillated Cellulose Nanofibril (CNF) Sheets with Increased Mechanical Performance for Use in High-Strength and Lightweight Structural and Packaging Applications. ACS Appl Polym Mater 1:2525–2534. https://doi.org/10.1021/acsapm.9b00635

Forti ES, Moon RJ, Schueneman GT, Youngblood JP (2020) Transparent tempo oxidized cellulose nanofibril (TOCNF) composites with increased toughness and thickness by lamination. Cellulose 1–17. https://doi.org/10.1007/s10570-020-03107-8

Fujisawa S, Okita Y, Fukuzumi H, et al (2011) Preparation and characterization of TEMPO-oxidized cellulose nanofibril films with free carboxyl groups. Carbohydr Polym 84:579–583. https://doi.org/10.1016/j.carbpol.2010.12.029

Fukuzumi H, Saito T, Iwata T, et al (2009) Transparent and high gas barrier films of cellulose nanofibers prepared by TEMPO-mediated oxidation. Biomacromolecules 10:162–165. https://doi.org/10.1021/bm801065u

Hakalahti M, Faustini M, Boissière C, et al (2017) Interfacial Mechanisms of Water Vapor Sorption into Cellulose Nanofibril Films as Revealed by Quantitative Models. Biomacromolecules 18:2951–2958. https://doi.org/10.1021/acs.biomac.7b00890

Iotti M, Gregersen ØW, Moe S, Lenes M (2011) Rheological Studies of Microfibrillar Cellulose Water Dispersions. J Polym Environ 19:137–145. https://doi.org/10.1007/s10924-010-0248-2

Isogai A, Saito T, Fukuzumi H (2011) TEMPO-oxidized cellulose nanofibers. Nanoscale 3:71–85. https://doi.org/10.1039/C0NR00583E

Iwatake A, Nogi M, Yano H (2008) Cellulose nanofiber-reinforced polylactic acid. Compos Sci Technol 68:2103–2106. https://doi.org/10.1016/j.compscitech.2008.03.006

Jonoobi M, Harun J, Mathew AP, Oksman K (2010) Mechanical properties of cellulose nanofiber (CNF) reinforced polylactic acid (PLA) prepared by twin screw extrusion. Compos Sci Technol 70:1742–1747. https://doi.org/10.1016/j.compscitech.2010.07.005

Khutoryanskaya O V., Khutoryanskiy V V., Pethrick RA (2005) Characterisation of Blends Based on Hydroxyethylcellulose and Maleic Acid-alt-Methyl Vinyl Ether. Macromol Chem Phys 206:1497–1510. https://doi.org/10.1002/macp.200500069

Kurihara T, Isogai A (2015) Mechanism of TEMPO-oxidized cellulose nanofibril film reinforcement with poly(acrylamide). Cellulose 22:2607–2617. https://doi.org/10.1007/s10570-015-0680-5

Lasseuguette E, Roux D, Nishiyama Y (2008) Rheological properties of microfibrillar suspension of TEMPO-oxidized pulp. Cellulose 15:425–433. https://doi.org/10.1007/s10570-007-9184-2

Li J, Wei L, Leng W, et al (2018) Fabrication and characterization of cellulose nanofibrils/epoxy nanocomposite foam. J Mater Sci 53:4949–4960. https://doi.org/10.1007/s10853-017-1652-y

Lin P, Clash C, Pearce EM, et al (1988) Solubility and miscibility of poly(ethyl oxazoline). J Polym Sci Part B Polym Phys 26:603–619. https://doi.org/10.1002/polb.1988.090260312

Liu D, Sun X, Tian H, et al (2013) Effects of cellulose nanofibrils on the structure and properties on PVA nanocomposites. Cellulose 20:2981–2989. https://doi.org/10.1007/s10570-013-0073-6

Liu P, Borrell PF, Božič M, et al (2015) Nanocelluloses and their phosphorylated derivatives for selective adsorption of Ag+, Cu2+ and Fe3+ from industrial effluents. J Hazard Mater 294:177–185. https://doi.org/10.1016/j.jhazmat.2015.04.001

Liu Z, Ge X, Lu Y, et al (2012) Effects of chitosan molecular weight and degree of deacetylation on the properties of gelatine-based films. Food Hydrocoll 26:311–317. https://doi.org/10.1016/j.foodhyd.2011.06.008

Lundahl MJ, Berta M, Ago M, et al (2018) Shear and extensional rheology of aqueous suspensions of cellulose nanofibrils for biopolymer-assisted filament spinning. Eur Polym J 109:367–378. https://doi.org/10.1016/j.eurpolymj.2018.10.006

Meija J, Bushell M, Couillard M, et al (2020) Particle Size Distributions for Cellulose Nanocrystals Measured by Transmission Electron Microscopy: An Interlaboratory Comparison. Anal Chem 92:38. https://doi.org/10.1021/acs.analchem.0c02805

Meng X, Bocharova V, Tekinalp H, et al (2018) Toughening of nanocelluose/PLA composites via bio-epoxy interaction: Mechanistic study. Mater Des 139:188–197. https://doi.org/10.1016/j.matdes.2017.11.012

Montes F, Fu T, Youngblood JP, et al (2020) Rheological impact of using cellulose nanocrystals (CNC) in cement pastes. Constr Build Mater 235:117497. https://doi.org/10.1016/j.conbuildmat.2019.117497

Moon RJ, Martini A, Nairn J, et al (2011) Cellulose nanomaterials review: structure, properties and nanocomposites. Chem Soc Rev 40:3941–3994. https://doi.org/10.1039/C0CS00108B

Naderi A, Lindström T, Pettersson T (2014) The state of carboxymethylated nanofibrils after homogenization-aided dilution from concentrated suspensions: A rheological perspective. Cellulose 21:2357–2368. https://doi.org/10.1007/s10570-014-0329-9

Nair SS, Kuo P-Y, Chen H, Yan N (2017) Investigating the effect of lignin on the mechanical, thermal, and barrier properties of cellulose nanofibril reinforced epoxy composite. Ind Crop Prod 100:208–217

Pääkko M, Ankerfors M, Kosonen H, et al (2007) Enzymatic hydrolysis combined with mechanical shearing and high-pressure homogenization for nanoscale cellulose fibrils and strong gels. Biomacromolecules 8:1934–1941. https://doi.org/10.1021/bm061215p

Rondo T, Sawatari C, St Manley RJ, Gray DG (1994) Characterization of Hydrogen Bonding in Cellulose-Synthetic Polymer Blend Systems with Regioselectively Substituted Methylcellulose

Roohani M, Habibi Y, Belgacem NM, et al (2008) Macromolecular Nanotechnology Cellulose whiskers reinforced polyvinyl alcohol copolymers nanocomposites. https://doi.org/10.1016/j.eurpolymj.2008.05.024

Rowe AA, Tajvidi M, Gardner DJ (2016) Thermal stability of cellulose nanomaterials and their composites with polyvinyl alcohol (PVA). J Therm Anal Calorim 126:1371–1386. https://doi.org/10.1007/s10973-016-5791-1

Saito T, Hirota M, Tamura N, et al (2009) Individualization of Nano-Sized Plant Cellulose Fibrils by Direct Surface Carboxylation Using TEMPO Catalyst under Neutral Conditions. Biomacromolecules 10:1992–1996. https://doi.org/10.1021/bm900414t

Saito T, Kimura S, Nishiyama Y, Isogai A (2007) Cellulose nanofibers prepared by TEMPO-mediated oxidation of native cellulose. Biomacromolecules 8:2485–2491. https://doi.org/10.1021/bm0703970

Saito T, Uematsu T, Kimura S, et al (2011) Self-aligned integration of native cellulose nanofibrils towards producing diverse bulk materials. Soft Matter 7:8804–8809. https://doi.org/10.1039/c1sm06050c

Sjöberg M, Bergström L, Larsson A, Sjöström E (1999) The effect of polymer and surfactant adsorption on the colloidal stability and rheology of kaolin dispersions. Colloids Surfaces A Physicochem Eng Asp 159:197–208. https://doi.org/10.1016/S0927-7757(99)00174-0

Velásquez-Cock J, Gómez H. BE, Posada P, et al (2018) Poly (vinyl alcohol) as a capping agent in oven dried cellulose nanofibrils. Carbohydr Polym 179:118–125. https://doi.org/10.1016/j.carbpol.2017.09.089

Zhang Y, Li X, Wei B (2018) Environment-friendly poly(2-ethyl-2-oxazoline) as an innovative consolidant for ancient wall paintings. Nanomaterials 8:. https://doi.org/10.3390/nano8090649

Figures

Figure 1

Photograph show the transparency of TOCNF + 15wt% PVA composites (left) and TOCNF + 15wt% PEOX composite (right)

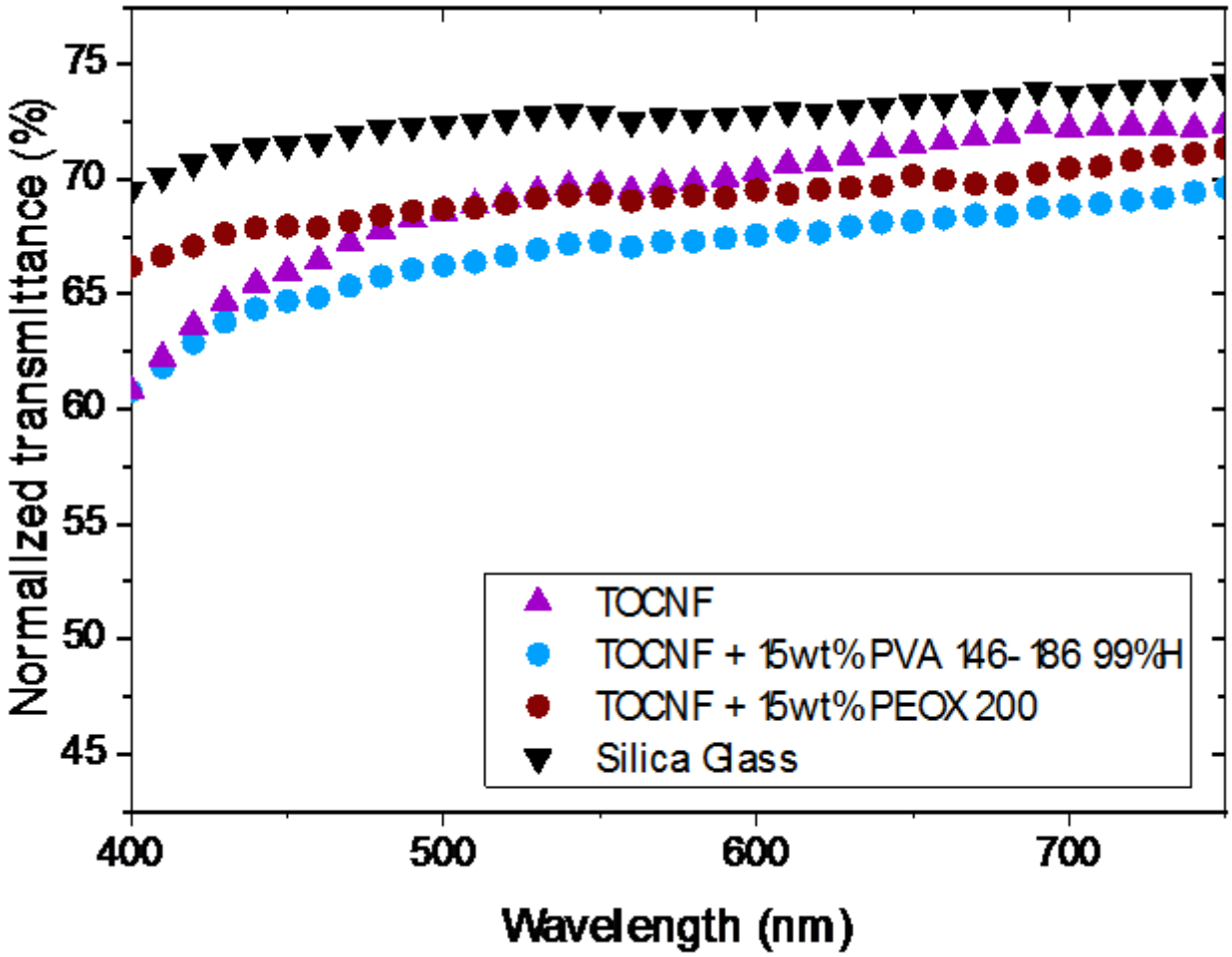

Figure 2

Visible transmittance via UV-Vis spectroscopy of neat TOCNF, TOCNF composites and silica glass. Thickness was normalized using the silica glass thickness as reference (0.9mm)

Image not available with this version

Figure 3

Image not available with this version

Figure 4

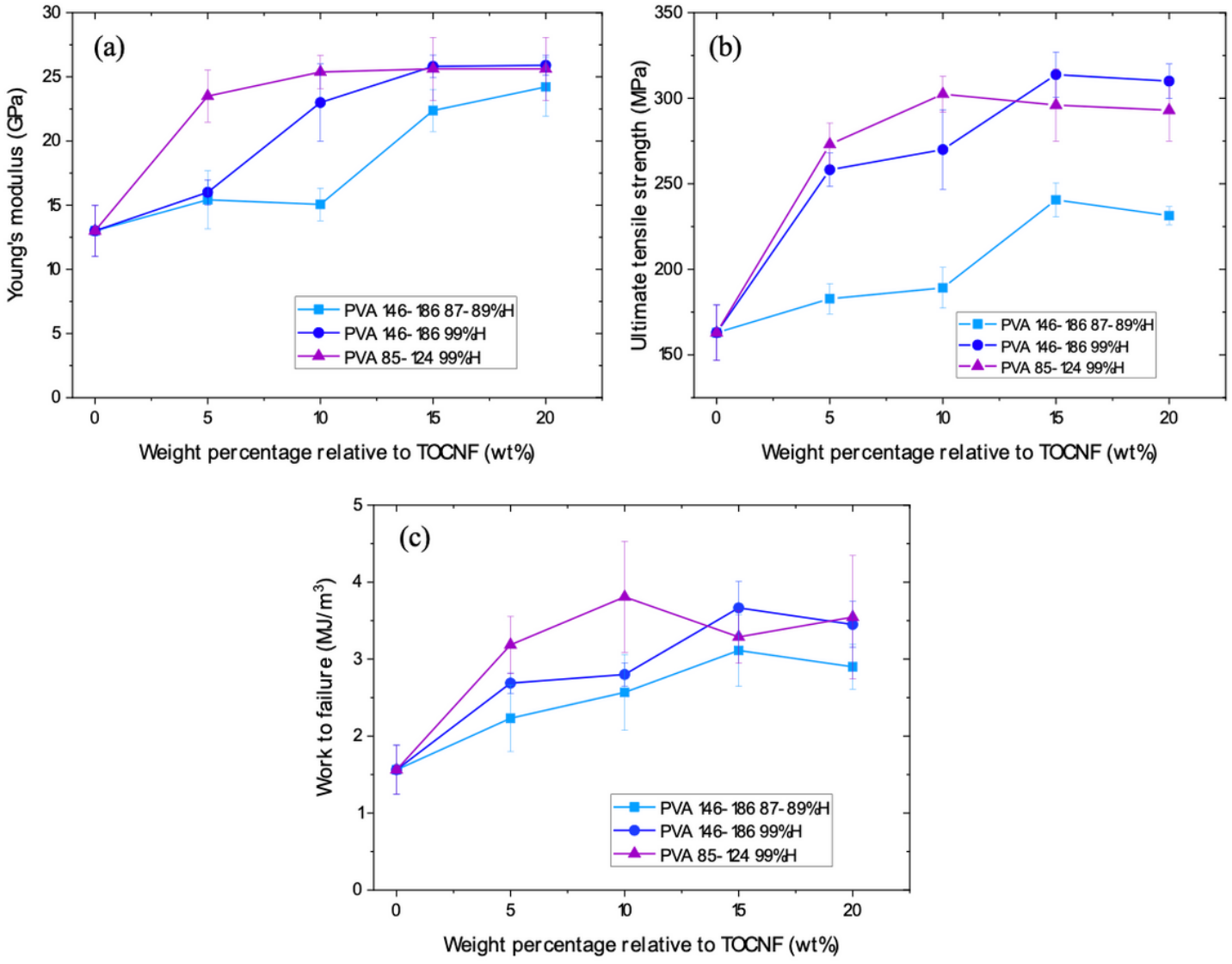

Figure 5

Tensile mechanical properties of c-TOCNF and PVA nanocomposites. (a) Young's modulus, (b) Ultimate Tensile Strength and (c) Work to failure

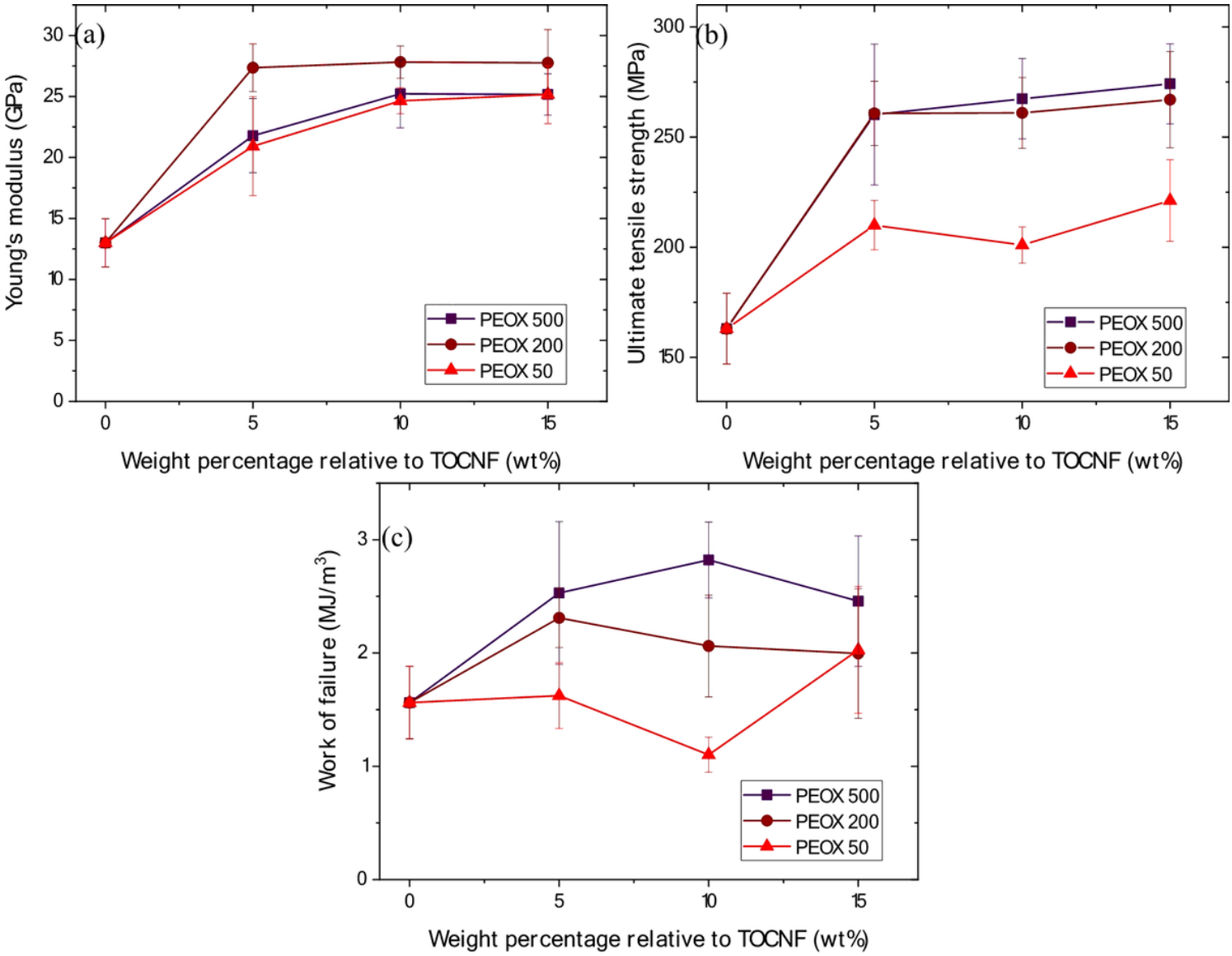

Figure 6

Tension properties of c-TOCNF and PEOX nanocomposites. (a) Young's modulus, (b) Ultimate Tensile Strength and (c) Work of failure

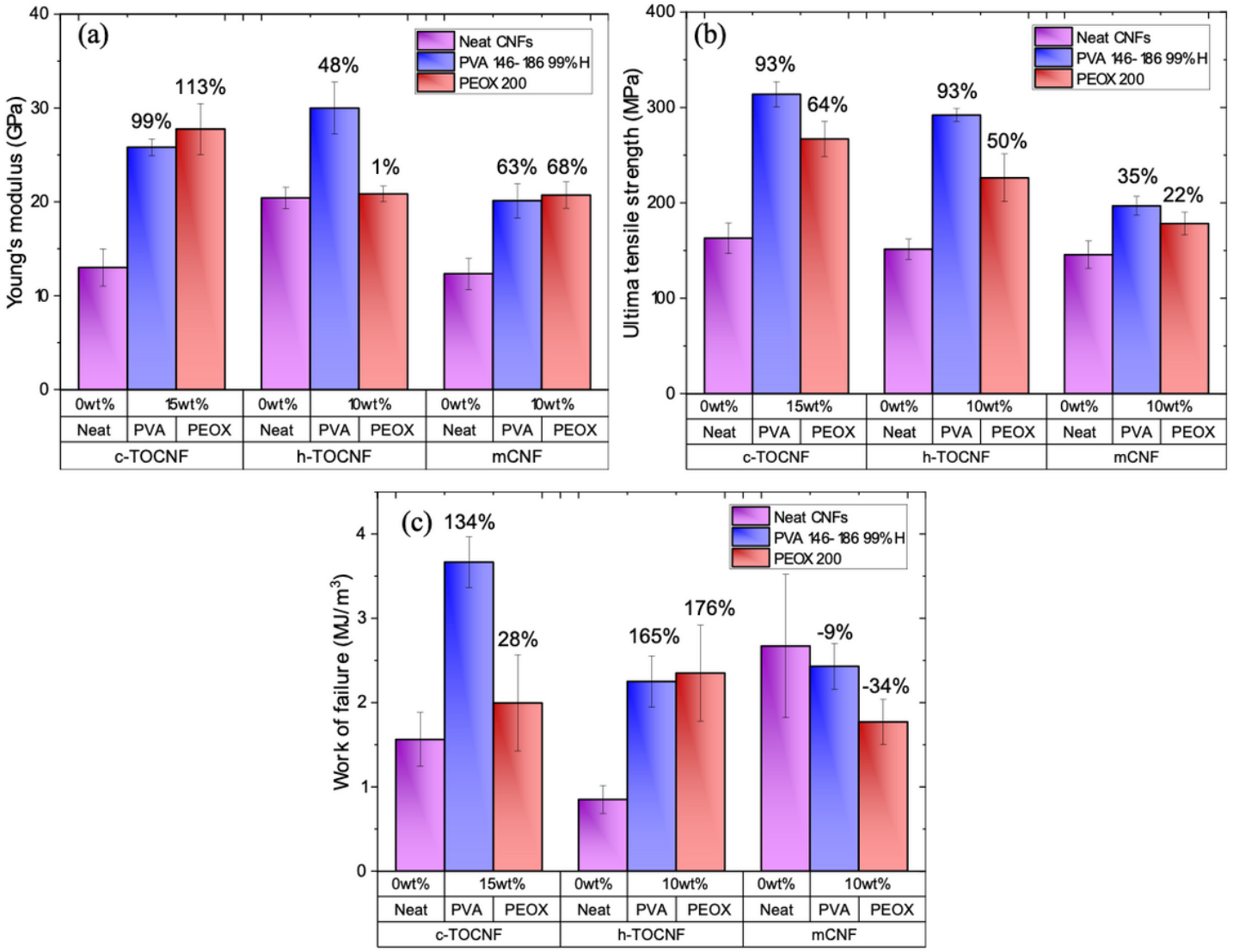

Figure 7

Mechanical response of different CNFs (c-TOCNF, h-TOCNF, mCNF) with different weight percentages of PVA and PEOX. (a) Young's Modulus, (b) Ultimate tensile strength (MPa) and (c) Work of failure.

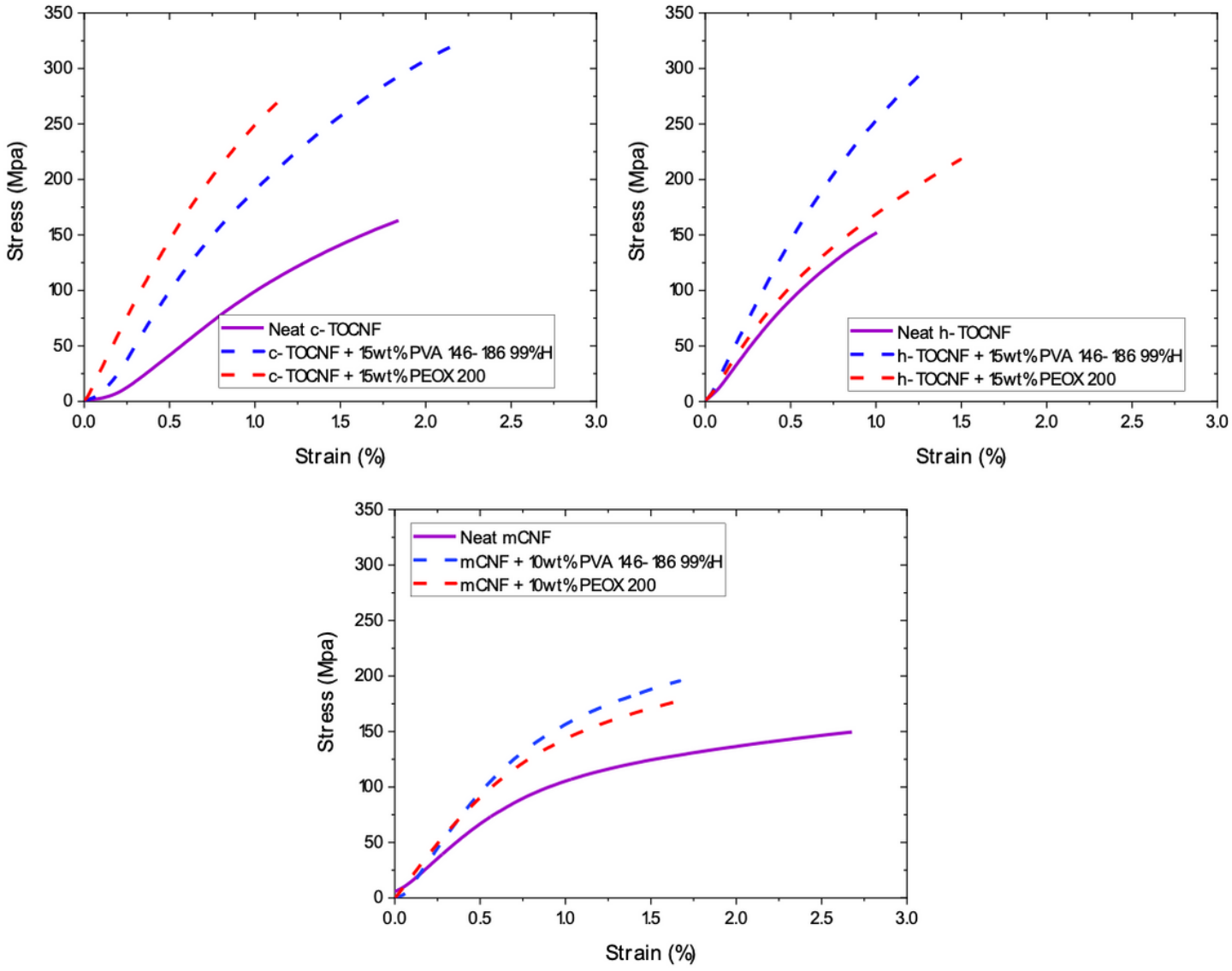

Figure 8

Representative stress-strain plots of neat and optimized PVA and PEO 200 composite c-TOCNF, h-TOCNF and mCNF films

Image not available with this version

Figure 9

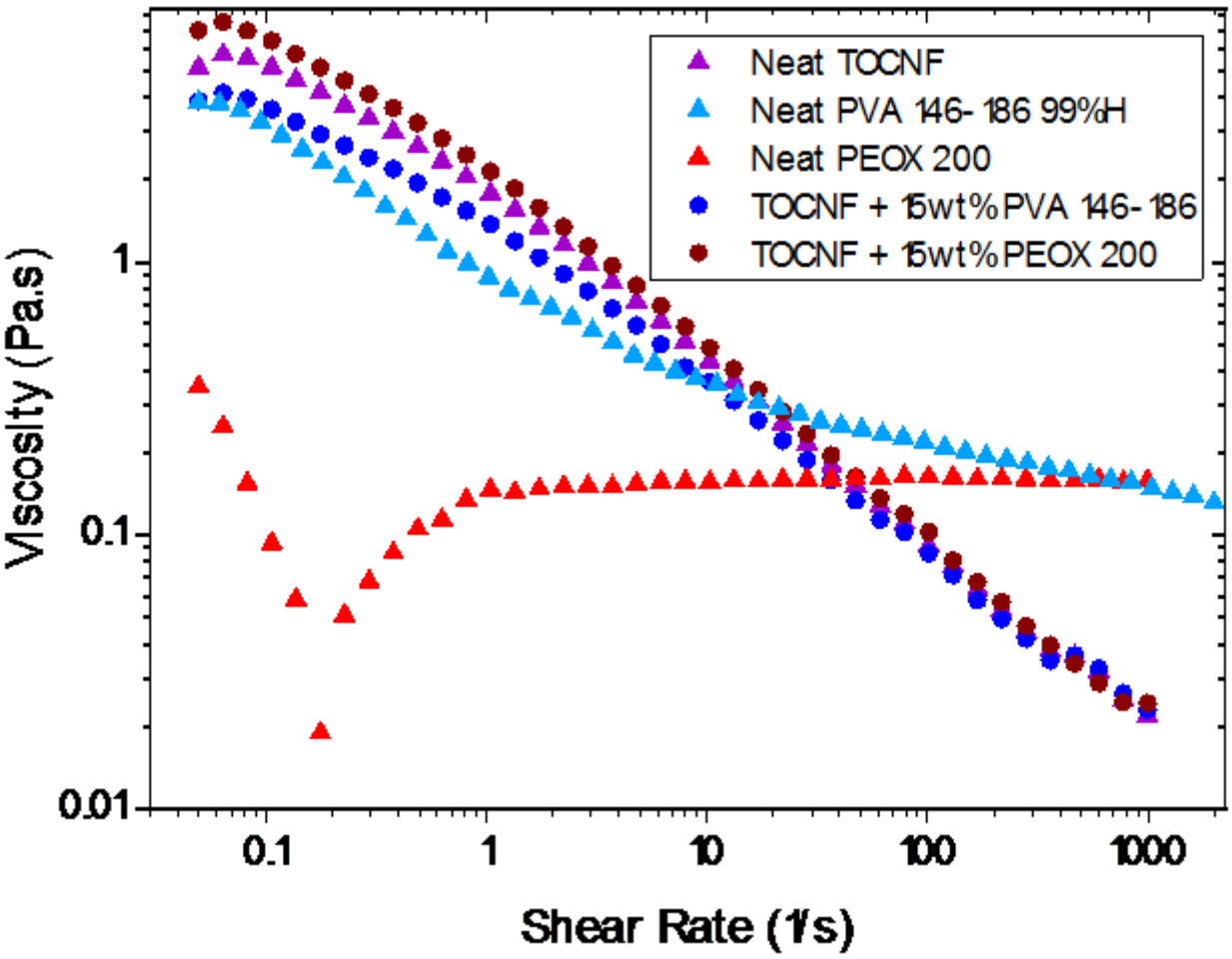

Figure 11

Rheology data for neat TOCNF, neat PVA 146-186 99%H, and neat PEOX 200 shown as triangular dots and composite fluids in circular dots. All TOCNF specimens are at constant 0.53 wt% TOCNF with any polymer added at 15 wt% to this

Supplementary Files

This is a list of supplementary files associated with this preprint. Click to download.

- GraphicalAbstract.png
- MechanicalEnhancementoffilmsSI.docx